Research Article | Vol. 30, No. 25 / 5 Dec 2022 / Optics Express 45212

Optics EXPRESS

Unveiling room temperature upconversion photoluminescence in monolayer WSe_2

AAMIR MUSHTAQ,[1] XIAODONG YANG,[1,3] AND JIE GAO[1,2,*]

[1]Department of Mechanical and Aerospace Engineering, Missouri University of Science and Technology, Rolla, MO 65409, USA
[2]Department of Mechanical Engineering, Stony Brook University, Stony Brook, NY 11794, USA
[3]yangxia@mst.edu
[*]jie.gao.5@stonybrook.edu

Abstract: Upconversion photoluminescence (UPL) is a phenomenon describing an anti-Stokes process where the emitted photons have higher energy than the absorbed incident photons. Transition metal dichalcogenides (TMDCs) with strong photon-exciton interactions represent a fascinating platform for studying the anti-Stokes UPL process down to the monolayer thickness limit. Herein, we demonstrate room-temperature UPL emission in monolayer WSe_2 with broadband near-infrared excitation. The measured excitation power dependence of UPL intensity at various upconversion energy gains unveils two distinguished upconversion mechanisms, including the one-photon involved multiphonon-assisted UPL process and the two-photon absorption (TPA) induced UPL process. In the phonon-assisted UPL regime, the observed exponential decay of UPL intensity with the increased energy gain is attributed to the decreased phonon population. Furthermore, valley polarization properties of UPL emission with circular polarization excitation is investigated. The demonstrated results will advance future photon upconversion applications based on monolayer TMDCs such as night vision, semiconductor laser cooling, and bioimaging.

1. Introduction

Photoluminescence (PL) is a light-matter interaction process in which low energy photons are emitted after the absorption of high energy photons, which normally obeys Stokes' law of luminescence [1]. Contrary to PL, upconversion photoluminescence (UPL) is an anti-Stokes process where the emitted photons have higher energy than the absorbed incident photons, due to additional energy gain triggered by series of other events like phonon participation [2] or multiphoton absorption [3,4]. During the UPL process, excitation photon ($\hbar\omega_{pump}$) couples to a real or virtual intermediate state and eventually results in photon emission at higher energy ($\hbar\omega_{emission}$) after gaining additional energy ΔE with energy conservation [5,6]. In solid-state systems, phonon-participated UPL process is a one-photon involved linear process, which is distinguished from other nonlinear optical processes such as two-photon absorption (TPA) induced PL and second-harmonic generation (SHG) emission [7]. UPL phenomena have been reported to occur efficiently in certain materials like organic dyes [4,6], rare-earth-doped materials [3], quantum wells [8] and quantum dots [9]. In recent years, UPL has attracted research interests due to its potential usefulness in varieties of applications such as photoluminescence bioimaging [10,11], photovoltaic energy conversion [12], lasers [13], displays [14] and optical refrigeration of solids [15].

Study of nanomaterials in the field of material science particularly two-dimensional (2D) materials has blossomed over the past years. Successful exfoliation of graphene with exceptional electrical [16], optical [17], thermal [18] and mechanical properties [19] flickered a trend on the exploration of 2D materials. 2D transition metal dichalcogenides (TMDCs) with chemical formula MX_2 (M = Mo, W, Re and X = S, Se, Te), where transition metal M is sandwiched

#471027 https://doi.org/10.1364/OE.471027
Journal © 2022 Received 19 Jul 2022; revised 22 Oct 2022; accepted 15 Nov 2022; published 29 Nov 2022

Optics EXPRESS

between two chalcogen X atoms, have emerged as vital materials for varied potential applications in electronics, optics and optoelectronics. Compared to substantially studied semiconductor materials, monolayer TMDCs have direct bandgaps with visible and near-infrared PL and much higher quantum efficiency [20–22]. In these confined low-dimensional systems, optical properties are dominated by excitons due to strong Coulomb binding effect. Benefiting from strong photon-exciton [23–25] and phonon-exciton [26,27] interactions, TMDCs at monolayer limit can be regarded as a promising platform beyond graphene for exploring UPL [28,29]. In monolayer TMDCs, TPA induced UPL in WSe_2 and multiphonon assisted UPL in WS_2 have been reported [30,31]. In addition, UPL is also reported in MoS_2 nanoflakes [32,33] and perovskites [34–36]. The detailed studies of the upconversion process in monolayer TMDCs operating at room temperature with broad bandwidth, as well as the upconversion mechanisms transitioning from one-photon to two-photon process, have not been explored extensively.

In this work, room-temperature UPL emission in chemical vapor deposition (CVD) grown WSe_2 monolayers with broadband near-infrared excitation wavelengths ranging from 785 to 950 nm is demonstrated. The excitation wavelength and power dependence of UPL spectra are measured and analyzed to unveil two distinguished mechanisms governing the upconversion processes, including the one-photon involved phonon-assisted UPL process and the TPA induced nonlinear UPL process. In the phonon-assisted regime, UPL with energy gain of up to 110 meV at room temperature has been obtained. The exponential decay of UPL intensity with the increased upconversion energy gain is observed due to the reduced phonon population. Furthermore, valley depolarization during UPL process is investigated with circular polarization excitation.

2. Characterization of UPL emission in monolayer WSe_2

Figure 1(a) depicts an optical reflection microscope image of the CVD grown WSe_2 monolayer triangles on sapphire substrate (2D Semiconductors). The PL and Raman spectra from monolayer WSe_2 shown in Fig. 1(b) and (c) are measured with a 632.8 nm He-Ne excitation laser by collecting the back reflected signal through a 40× objective lens (NA = 0.65) and an edge filter (Semrock, LP02-633RE-25) and coupling into a spectrometer (Horiba, iHR 550). Figure 1(b) indicates that the PL emission of monolayer WSe_2 is centered around 760 nm at room temperature. Figure 1(c) infers that two main Raman peaks are obtained in the 100-300 cm^{-1} frequency range for monolayer WSe_2. The Raman peak at 125 cm^{-1} corresponds to the longitudinal acoustic (LA) phonon mode, while the peak at 246 cm^{-1} represents both the in-plane $E^1{}_{2g}$ and out-of-plane A_{1g} phonon modes appearing around 250 cm^{-1} (with phonon energy of 31 meV), which is consistent with the previously reported values [37].

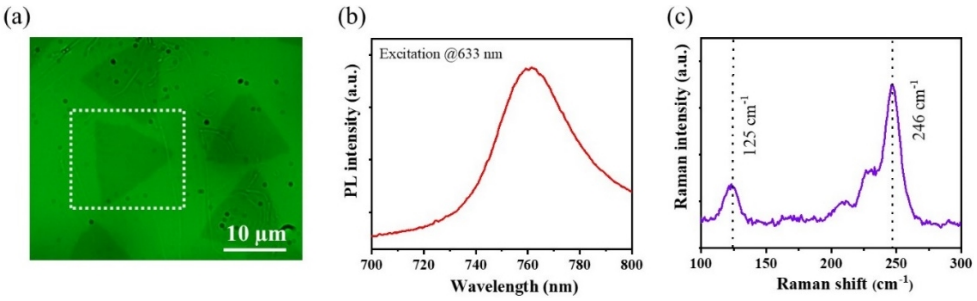

Fig. 1. (a) Optical reflection microscope image of the CVD grown WSe_2 monolayer triangles. (b), (c) Measured PL and Raman spectra of monolayer WSe_2.

Next, in order to study the excitation photon energy dependence of the upconversion emission at room temperature, the UPL spectra from monolayer WSe_2 are measured with tunable near-infrared

Optics EXPRESS

excitation wavelength from 785 to 950 nm using a Ti:Sapphire laser (Coherent Chameleon) and a set of short-pass filters. As displayed in Fig. 2, the collected UPL spectra are always peaked at the excitonic transition of monolayer WSe_2 around 760 nm (1.63 eV) for all the excitation wavelengths, which is consistent with the measured down-conversion PL peak energy. It is noted that only half UPL spectra are presented for excitation wavelengths shorter than 815 nm with a 775 nm short-pass filter, while full UPL spectra are exhibited for longer excitation wavelengths.

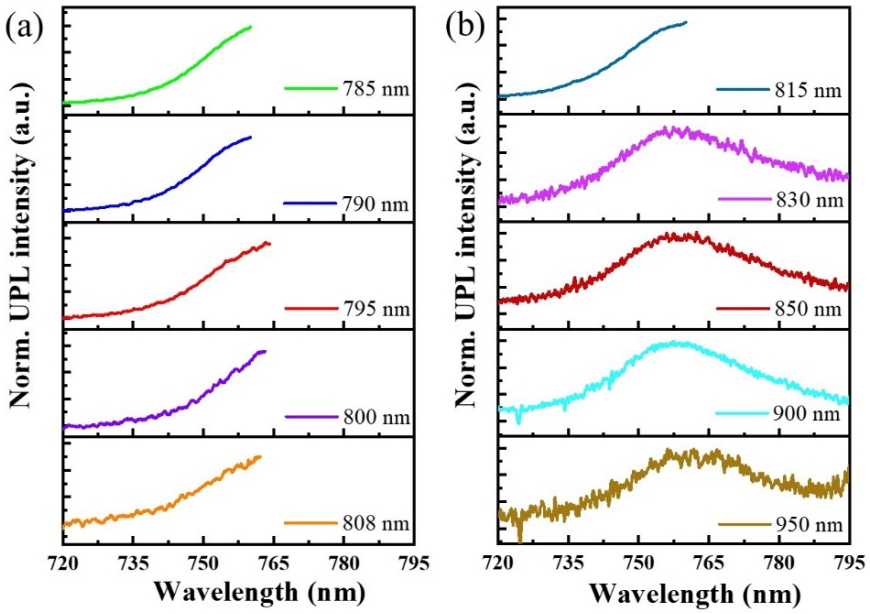

Fig. 2. Measured UPL spectra from monolayer WSe_2 as a function of the excitation wavelength from 785 to 950 nm.

In order to unveil the underlying mechanism of the UPL process, the excitation power dependence of the upconversion emission at each excitation wavelength is investigated. Figure 3(a) and (b) plot the measured UPL spectra at the excitation wavelengths of 785 and 815 nm under different excitation powers. It shows that the UPL intensity increases with the variation of excitation power, while the UPL spectra almost maintain the same shape. Figure 3(c) summaries the detailed power dependence of the UPL intensity in a log-log scale for all the excitation wavelengths. The UPL intensity is fitted to the power law $I = \alpha P^{\beta}$, where P is the excitation power, α is a fitting parameter, and β is the exponent of the power law which represents the slope of the curve. It is observed that the slope becomes steeper with increasing excitation wavelength. At a certain level of UPL intensity, a higher excitation power is required at the longer excitation wavelength. The extracted value of β as a function of the corresponding excitation wavelength is further plotted in Fig. 3(d). It is inferred that β value is close to 1.0 when the excitation wavelength is below 800 nm, indicating the linear power dependence of the one-photon involved phonon-assisted UPL process. As the excitation wavelength keeps increasing till 815 nm, the β value increases to around 1.3, showing the UPL process enters into a transition region to the two-photon process. Afterwards, as the excitation wavelength goes up to 950 nm, the β value increases from 1.5 to 2.3, manifesting the nonlinear power dependence of the multiphoton absorption induced UPL process. The behavior of β value indicates two distinguished mechanisms governing the UPL process at room temperature. In the one-photon regime with $\beta \sim 1$, UPL is dominated by one photon excitation followed by absorbing additional

Optics EXPRESS

phonon energy. On the other hand, in the two-photon regime with $\beta \sim 2$, UPL is governed by the superlinear TPA induced emission process.

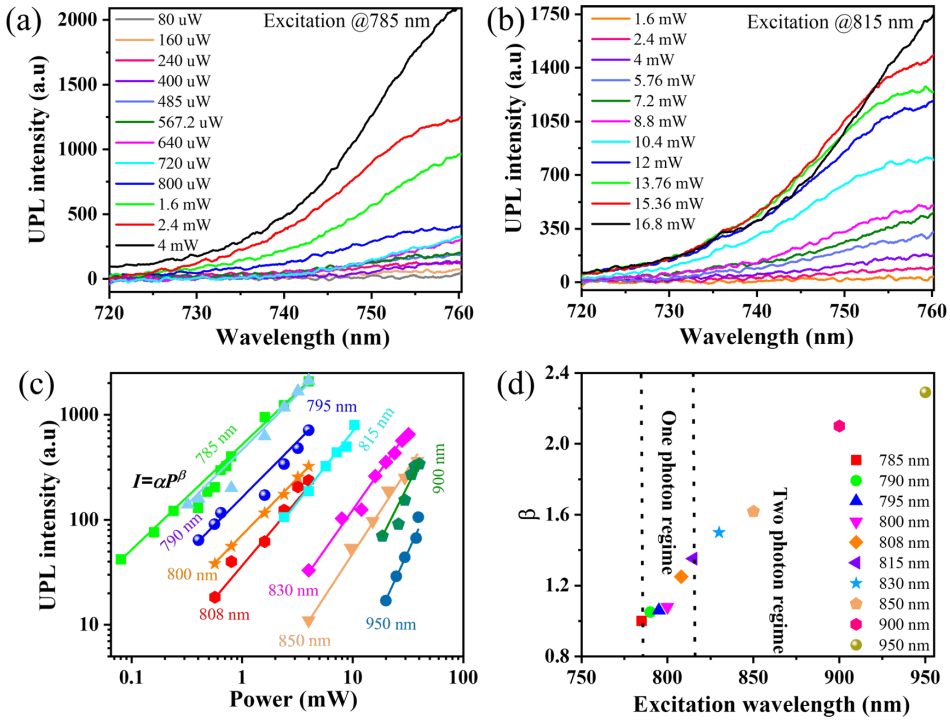

Fig. 3. (a), (b) Recorded excitation power-dependent UPL spectra at the excitation wavelengths of 785 and 815 nm, respectively. (c) Power dependence of the UPL intensity at different excitation wavelengths. The measured data are presented by the solid dots, while the colored solid lines show the fittings to the power law. (d) Extracted value of β as a function of the excitation wavelength, depicting one-photon and two-photon regimes.

The schematic representation of the above-mentioned two underlying mechanisms for the UPL processes is shown in Fig. 4. For the general PL process, the above-bandgap excitation will result in the generation of excitons which subsequently relax to the band edge followed by the excitonic photon emission with the radiative recombination, with the energy centered at 760 nm (1.63 eV). However, for the observed UPL phenomena, the excitonic emission also occurs when the excitation energy is tuned below the bandgap. Figure 4(a) depicts the one-photon involved phonon-assisted UPL process, where it is speculated that the excitonic emission is mediated by phonons coupled to an intermediate state followed by the relaxation to the band edge, taking into account both momentum and energy conversation during the UPL process [29,38,39]. In contrast, Fig. 4(b) explains the TPA induced UPL process via a virtual state as a nonlinear optical process.

To further understand the multiphonon-assisted UPL process in monolayer WSe_2, the excitation photon energy dependence of the upconversion emission is studied. Figure 5(a) and (b) display the measured UPL spectra under two excitation powers of 1.6 and 2.4 mW at different excitation wavelengths from 785 to 815 nm, corresponding to the upconversion energy gain ΔE of 50 to 110 meV. It can be seen that the UPL intensity drops dramatically with increasing excitation wavelength. As the excitation wavelength varies, the spectral shape and peak position remain intact, which rules out the possibility of UPL from anti-Stokes Raman scattering. Furthermore, the integrated UPL intensity as a function of the energy gain is plotted in Fig. 5(c) and (d), where a

Optics EXPRESS

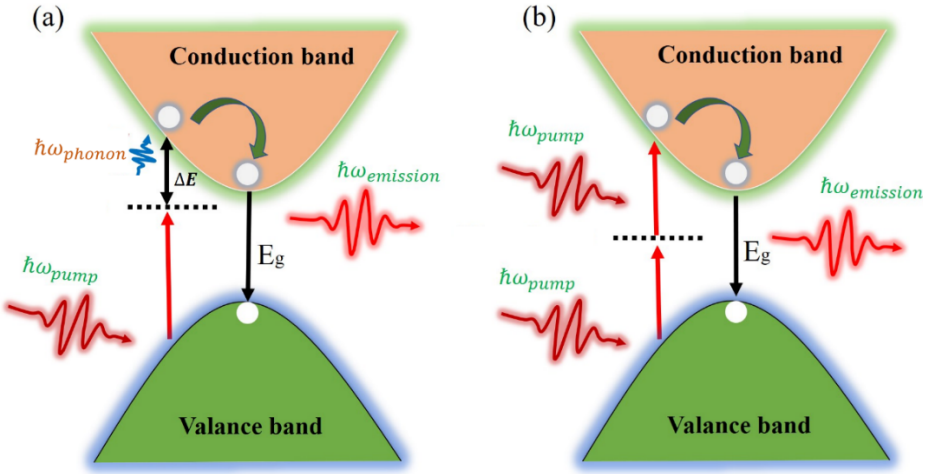

Fig. 4. Schematic representation of two underlying mechanisms responsible for the UPL processes.

clear exponential decay of the UPL intensity is observed due to the decreased phonon population. For both excitation powers, the experimental data are well fitted by the Boltzmann distribution function $I = I_0 \exp(-\Delta E/k_B T)$ [40], where I is the UPL intensity, k_B is the Boltzmann constant, T is the room temperature, and $\Delta E = \hbar\omega_{emission} - \hbar\omega_{pump}$ is the upconversion energy gain. It is found that the involved phonon number $n = \Delta E/\hbar\omega_{phonon}$ ranges from 2 to 4 in the measured multiphonon-assisted UPL process, by comparing the observed energy gain with the phonon energy $\hbar\omega_{phonon}$ of 31 meV for the out-of-plane A_{1g} phonon modes in monolayer WSe_2.

Moreover, the circular polarization dependence of the multiphonon-assisted UPL emission as a function of the upconversion energy gain is investigated to show the influence of the off-resonance excitation on the valley properties in monolayer WSe_2. Figures 6(a)-(d) plot the left-handed and right-handed circular polarization (LCP, $\sigma+$ and RCP, $\sigma-$) components of the UPL spectra under RCP excitation at different wavelengths from 785 to 800 nm, corresponding to the upconversion energy gain of 50 to 80 meV. The valley polarization of excitons during the upconversion can be indicated by the degree of polarization (DOP), which is defined by $\text{DOP} = (I_{\sigma_-} - I_{\sigma+})/(I_{\sigma_-} + I_{\sigma+})$ [41], with $I_{\sigma+}$ and I_{σ_-} as the LCP and RCP components of the UPL intensity. Figure 6(e) presents the DOP evaluated at the UPL emission peak at each excitation wavelength. It shows that the DOP value reduces quickly as the energy gain is increased, following a linear function with a slope of $-0.00416\ \text{meV}^{-1}$. It is inferred that the valley depolarization process of excitons gets stronger as the excitation energy is away from the excitonic resonance.

Optics EXPRESS

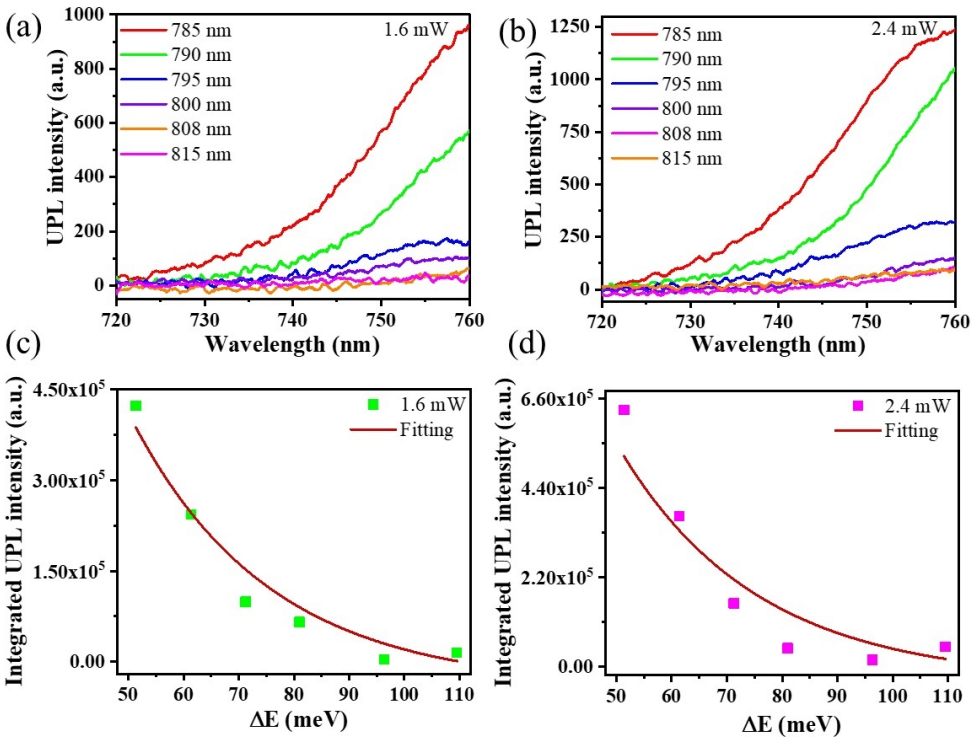

Fig. 5. (a), (b) Measured UPL spectra at different excitation wavelengths from 785 to 815 nm under two excitation powers of 1.6 and 2.4 mW, respectively. (c), (d) Integrated UPL intensity as a function of the energy gain under the corresponding excitation power. The measured data are shown by the solid squares, while the solid curves represent the exponential fittings.

Optics EXPRESS

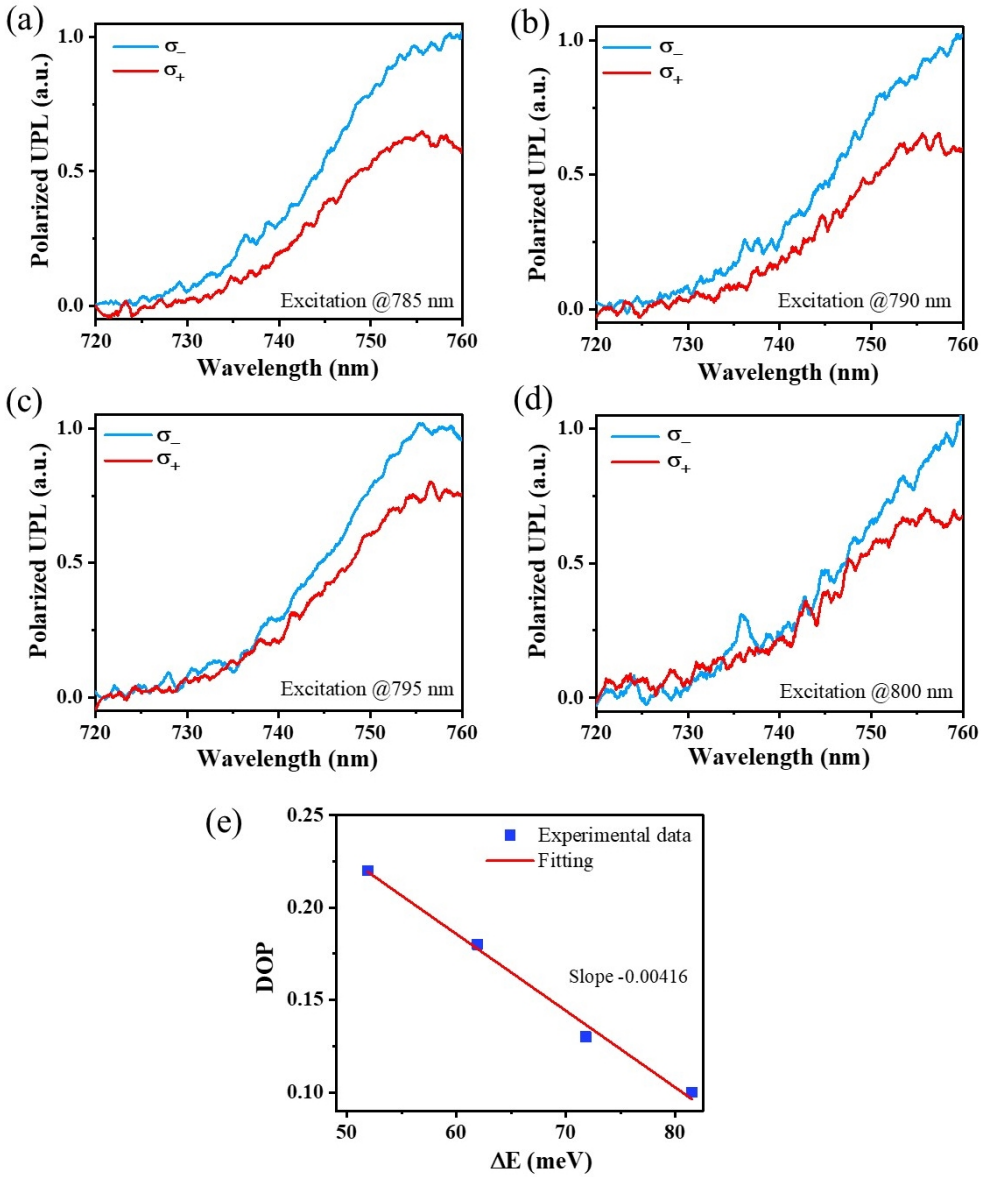

Fig. 6. (a)-(d) Measured circular polarization-resolved UPL spectra at different excitation wavelengths. (e) DOP value as a function of the energy gain.

Optics EXPRESS

3. Conclusion

In conclusion, we have demonstrated room-temperature UPL emission in monolayer WSe_2 at broadband near-infrared excitation wavelengths with the upconversion energy gain of up to 326 meV. By analyzing the excitation wavelength and power dependent UPL spectra, two distinguished mechanisms governing the upconversion processes are unveiled as the one-photon involved multiphonon-assisted UPL process and the TPA induced nonlinear UPL process. The energy gain of up to 110 meV has been achieved for the multiphonon-assisted UPL emission at room temperature. The observed exponential decay of UPL intensity with increasing energy gain originates from the reduced phonon population. In addition, valley depolarization during UPL process has also been revealed by the circular polarization-resolved measurements. The phonon-assisted upconversion process involves the photon absorption of intermediate states and the interaction with optical phonons, therefore the increase in the intermediate state density and the phonon population density will improve the upconversion efficiency. We envision that the demonstrated UPL processes in 2D materials will open new vista for the advancement of future photon upconversion technologies in photovoltaics, night vision, laser cooling, and bioimaging.

Funding. Defense Advanced Research Projects Agency (W911NF2110353).

Disclosures. The authors declare no conflicts of interest.

Data availability. Data underlying the results presented in this paper are not publicly available at this time but may be obtained from the authors upon reasonable request.

References

1. G. G. Stokes, "On the change of refrangibility of light," Philos. Trans. R. Soc. Lond. **142**, 267–414 (1852).
2. M. Sheik-Bahae and R. I. Epstein, "Optical refrigeration," Nat. Photonics **1**(12), 693–699 (2007).
3. F. Auzel, "Upconversion and Anti-Stokes Processes with f and d Ions in Solids," Chem. Rev. **104**(1), 139–174 (2004).
4. J. Zhao, S. Ji, and H. Guo, "Triplet–triplet annihilation based upconversion: from triplet sensitizers and triplet acceptors to upconversion quantum yields," RSC Adv. **1**(6), 937–950 (2011).
5. B. Zhou, B. Shi, D. Jin, and X. Liu, "Controlling upconversion nanocrystals for emerging applications," Nat. Nanotechnol. **10**(11), 924–936 (2015).
6. S. Baluschev, T. Miteva, V. Yakutkin, G. Nelles, A. Yasuda, and G. Wegner, "Up-Conversion Fluorescence: Noncoherent Excitation by Sunlight," Phys. Rev. Lett. **97**(14), 143903 (2006).
7. M. Wu, D. N. Congreve, M. W. B. Wilson, J. Jean, N. Geva, M. Welborn, T. Van Voorhis, V. Bulović, M. G. Bawendi, and M. A. Baldo, "Solid-state infrared-to-visible upconversion sensitized by colloidal nanocrystals," Nat. Photonics **10**(1), 31–34 (2016).
8. G. Bacher, C. Hartmann, H. Schweizer, T. Held, G. Mahler, and H. Nickel, "Exciton dynamics in $In_xGa_{1-x}As$/GaAs quantum-well heterostructures: Competition between capture and thermal emission," Phys. Rev. B **47**(15), 9545–9555 (1993).
9. Z. Deutsch, L. Neeman, and D. Oron, "Luminescence upconversion in colloidal double quantum dots," Nat. Nanotechnol. **8**(9), 649–653 (2013).
10. C. Vinegoni, D. Razansky, S. A. Hilderbrand, F. Shao, V. Ntziachristos, and R. Weissleder, "Transillumination fluorescence imaging in mice using biocompatible upconverting nanoparticles," Opt. Lett. **34**(17), 2566–2568 (2009).
11. C. T. Xu, N. Svensson, J. Axelsson, P. Svenmarker, G. Somesfalean, G. Chen, H. Liang, H. Liu, Z. Zhang, and S. Andersson-Engels, "Autofluorescence insensitive imaging using upconverting nanocrystals in scattering media," Appl. Phys. Lett. **93**(17), 171103 (2008).
12. V. Gray, D. Dzebo, M. Abrahamsson, B. Albinsson, and K. Moth-Poulsen, "Triplet–triplet annihilation photon-upconversion: towards solar energy applications," Phys. Chem. Chem. Phys. **16**(22), 10345–10352 (2014).
13. G. S. He, P. P. Markowicz, T.-C. Lin, and P. N. Prasad, "Observation of stimulated emission by direct three-photon excitation," Nature **415**(6873), 767–770 (2002).
14. E. Downing, L. Hesselink, J. Ralston, and R. Macfarlane, "A Three-Color, Solid-State, Three-Dimensional Display," Science **273**(5279), 1185–1189 (1996).
15. R. I. Epstein, M. I. Buchwald, B. C. Edwards, T. R. Gosnell, and C. E. Mungan, "Observation of laser-induced fluorescent cooling of a solid," Nature **377**(6549), 500–503 (1995).
16. J.-H. Chen, C. Jang, S. Xiao, M. Ishigami, and M. S. Fuhrer, "Intrinsic and extrinsic performance limits of graphene devices on SiO_2," Nat. Nanotechnol. **3**(4), 206–209 (2008).
17. F. Bonaccorso, Z. Sun, T. Hasan, and A. C. Ferrari, "Graphene photonics and optoelectronics," Nat. Photonics **4**(9), 611–622 (2010).
18. E. Pop, V. Varshney, and A. K. Roy, "Thermal properties of graphene: Fundamentals and applications," MRS Bull. **37**(12), 1273–1281 (2012).

Optics EXPRESS

19. C. Lee, X. Wei, J. W. Kysar, and J. Hone, "Measurement of the Elastic Properties and Intrinsic Strength of Monolayer Graphene," Science **321**(5887), 385–388 (2008).
20. Q. H. Wang, K. Kalantar-Zadeh, A. Kis, J. N. Coleman, and M. S. Strano, "Electronics and optoelectronics of two-dimensional transition metal dichalcogenides," Nat. Nanotechnol. **7**(11), 699–712 (2012).
21. K. F. Mak, C. Lee, J. Hone, J. Shan, and T. F. Heinz, "Atomically Thin MoS_2: A New Direct-Gap Semiconductor," Phys. Rev. Lett. **105**(13), 136805 (2010).
22. J. Wang, H. Li, Y. Ma, M. Zhao, W. Liu, B. Wang, S. Wu, X. Liu, L. Shi, T. Jiang, and J. Zi, "Routing valley exciton emission of a WS_2 monolayer via delocalized Bloch modes of in-plane inversion-symmetry-broken photonic crystal slabs," Light: Sci. Appl. **9**(1), 148 (2020).
23. J. Shi, Y. Li, Z. Zhang, W. Feng, Q. Wang, S. Ren, J. Zhang, W. Du, X. Wu, X. Sui, Y. Mi, R. Wang, Y. Sun, L. Zhang, X. Qiu, J. Lu, C. Shen, Y. Zhang, Q. Zhang, and X. Liu, "Twisted-Angle-Dependent Optical Behaviors of Intralayer Excitons and Trions in WS_2/WSe_2 Heterostructure," ACS Photonics **6**(12), 3082–3091 (2019).
24. B. Wen, Y. Zhu, D. Yudistira, A. Boes, L. Zhang, T. Yidirim, B. Liu, H. Yan, X. Sun, Y. Zhou, Y. Xue, Y. Zhang, L. Fu, A. Mitchell, H. Zhang, and Y. Lu, "Ferroelectric-Driven Exciton and Trion Modulation in Monolayer Molybdenum and Tungsten Diselenides," ACS Nano **13**(5), 5335–5343 (2019).
25. K. F. Mak, K. He, J. Shan, and T. F. Heinz, "Control of valley polarization in monolayer MoS_2 by optical helicity," Nat. Nanotechnol. **7**(8), 494–498 (2012).
26. J. Jadczak, A. Delgado, L. Bryja, Y. S. Huang, and P. Hawrylak, "Robust high-temperature trion emission in monolayers of $Mo(S_ySe_{1-y})_2$alloys," Phys. Rev. B **95**(19), 195427 (2017).
27. K. Kaasbjerg, K. S. Thygesen, and K. W. Jacobsen, "Phonon-limited mobility in n-type single-layer MoS_2 from first principles," Phys. Rev. B **85**(11), 115317 (2012).
28. J. He, L. Tao, H. Zhang, B. Zhou, and J. Li, "Emerging 2D materials beyond graphene for ultrashort pulse generation in fiber lasers," Nanoscale **11**(6), 2577–2593 (2019).
29. A. M. Jones, H. Yu, J. R. Schaibley, J. Yan, D. G. Mandrus, T. Taniguchi, K. Watanabe, H. Dery, W. Yao, and X. Xu, "Excitonic luminescence upconversion in a two-dimensional semiconductor," Nat. Phys. **12**(4), 323–327 (2016).
30. M. Manca, M. M. Glazov, C. Robert, F. Cadiz, T. Taniguchi, K. Watanabe, E. Courtade, T. Amand, P. Renucci, X. Marie, G. Wang, and B. Urbaszek, "Enabling valley selective exciton scattering in monolayer WSe_2 through upconversion," Nat. Commun. **8**(1), 14927 (2017).
31. J. Jadczak, L. Bryja, J. Kutrowska-Girzycka, P. Kapuściński, M. Bieniek, Y. S. Huang, and P. Hawrylak, "Room temperature multi-phonon upconversion photoluminescence in monolayer semiconductor WS_2," Nat. Commun. **10**(1), 107 (2019).
32. X. Dai, X. Zhang, I. M. Kislyakov, L. Wang, J. Huang, S. Zhang, N. Dong, and J. Wang, "Enhanced two-photon absorption and two-photon luminescence in monolayer MoS_2 and WS_2 by defect repairing," Opt. Express **27**(10), 13744–13753 (2019).
33. Y. Li, N. Dong, S. Zhang, X. Zhang, Y. Feng, K. Wang, L. Zhang, and J. Wang, "Giant two-photon absorption in monolayer MoS_2," Laser Photonics Rev. **9**(4), 427–434 (2015).
34. K. Mase, K. Okumura, N. Yanai, and N. Kimizuka, "Triplet sensitization by perovskite nanocrystals for photon upconversion," Chem. Commun. **53**(59), 8261–8264 (2017).
35. S. Wieghold and L. Nienhaus, "Precharging Photon Upconversion: Interfacial Interactions in Solution-Processed Perovskite Upconversion Devices," J. Phys. Chem. Lett. **11**(3), 601–607 (2020).
36. A. Mushtaq, B. Pradhan, D. Kushavah, Y. Zhang, M. Wolf, N. Schrenker, E. Fron, S. Bals, J. Hofkens, E. Debroye, and S. K. Pal, "Third-Order Nonlinear Optical Properties and Saturation of Two-Photon Absorption in Lead-Free Double Perovskite Nanocrystals under Femtosecond Excitation," ACS Photonics **8**(11), 3365–3374 (2021).
37. Z. Chu, A. Han, C. Lei, S. Lopatin, P. Li, D. Wannlund, D. Wu, K. Herrera, X. Zhang, A. H. MacDonald, X. Li, L.-J. Li, and K. Lai, "Energy-Resolved Photoconductivity Mapping in a Monolayer–Bilayer WSe_2 Lateral Heterostructure," Nano Lett. **18**(11), 7200–7206 (2018).
38. R. Hellmann, A. Euteneuer, S. G. Hense, J. Feldmann, P. Thomas, E. O. Göbel, D. R. Yakovlev, A. Waag, and G. Landwehr, "Low-temperature anti-Stokes luminescence mediated by disorder in semiconductor quantum-well structures," Phys. Rev. B **51**(24), 18053–18056 (1995).
39. Y. P. Rakovich, A. A. Gladyshchuk, K. I. Rusakov, S. A. Filonovich, M. J. M. Gomes, D. V. Talapin, A. L. Rogach, and A. Euchmüller, "Anti-Stokes Luminescence of Cadmium Telluride Nanocrystals," J. Appl. Spectrosc. **69**(3), 444–449 (2002).
40. Q. Wang, Q. Zhang, X. Zhao, Y. J. Zheng, J. Wang, X. Luo, J. Dan, R. Zhu, Q. Liang, L. Zhang, P. K. J. Wong, X. He, Y. L. Huang, X. Wang, S. J. Pennycook, G. Eda, and A. T. S. Wee, "High-Energy Gain Upconversion in Monolayer Tungsten Disulfide Photodetectors," Nano Lett. **19**(8), 5595–5603 (2019).
41. P. K. Nayak, F.-C. Lin, C.-H. Yeh, J.-S. Huang, and P.-W. Chiu, "Robust room temperature valley polarization in monolayer and bilayer WS_2," Nanoscale **8**(11), 6035–6042 (2016).